Journal of Environmental Chemical Engineering 8 (2020) 104128

Contents lists available at ScienceDirect

Journal of Environmental Chemical Engineering

journal homepage: www.elsevier.com/locate/jece

Physicochemical modifications of radioactive oil sludge by ozone treatment

Leandro Goulart de Araujo[a,*], Eduardo Sant'Ana Petraconi Prado[a], Felipe de Souza Miranda[b], Roberto Vicente[a], Argemiro Soares da Silva Sobrinho[b], Gilberto Petraconi Filho[b], Júlio Takehiro Marumo[a]

[a] Nuclear and Energy Research Institute, Av. Prof. Lineu Prestes, 2242 – Cidade Universitária, São Paulo, SP, 05508-900, Brazil
[b] Technological Institute of Aeronautics, LPP/ITA, Praça Mal. Eduardo Gomes, 50 – Vila das Acácias, São José dos Campos, SP, 12228-900, Brazil

ARTICLE INFO

Editor: G.L. Dotto

Keywords:
Radioactive oil sludge
Ozone
Advanced oxidation process
Physicochemical modifications
FTIR
Residual gas analysis

ABSTRACT

An experimental study on the degradation of organic compounds from radioactive oil sludge by the ozonation process is presented. The effects of different concentrations of ozone in the oil sludge degradation over time were investigated. The experiments were performed in a 0.125 L glass reactor with magnetic stirring and a diffuser plate at the bottom to feed the ozone. The ozone concentration varied from 13 to 53 mg L^{-1} and the total interaction time was 1 h. To investigate the physicochemical properties of the oil sludge (solid and liquid components) prior to and after the treatment, multiple analytical characterization methods were used: Thermal Gravimetric Analysis, X-ray diffraction, Scanning Electron Microscopy coupled with Energy-Dispersive X-ray Spectroscopy, Fourier Transform Infrared spectroscopy, Spectrophotometer, and Residual Gas Analyzer. The most perceptive change is in the color of the liquid medium turned from dark brown to light yellow, especially under ozone concentrations higher than 33 mg L^{-1}. Absorbance values decreased about 3.5 times after 30 min of treatment with $[O_3]$ = 53 mg L^{-1}. FTIR spectroscopy showed that the bands associated with the CH_3 and C—H in CH_2 disappeared during treatment. On the other hand, a greater presence of C=C aromatics was observed. By residual gas analysis, various organic and inorganic gases were identified during the treatment, such as CH_4, H_2, CO_2, and H_2S. Finally, the ozonation of the oil sludge proved to be effective, due to its high reaction capacity.

1. Introduction

Oil sludge containing Naturally Occurring Radioactive Materials (NORM) is often produced in oil platforms by accumulation in crude oil tanks, desalters, and elsewhere during oil production by two mechanisms: incorporation or precipitation in the use of industrial equipment [1]. Oil sludge is a mixture of oil, water, and sediment that accumulate inside pipes, tanks, and other rigging equipment. It may contain radionuclides from the natural radioactive series of thorium and uranium, in addition to Potassium-40 [2].

The interest in the development of treatment methods for this type of waste is increasing worldwide since it cannot be disposed of as landfill and its accumulation in large quantities and with significant levels of activity represents an economic burden and a licensing issue for long term storage. Above all, it can cause concerns about environmental pollution and health risks for workers and the local population [3]. In this context, some treatment methods have been proposed for further application on oil production networks. The most used are conventional technologies, such as biological treatment, incineration, etc. [4].

Jing et al. [5] compared these treatments in terms of effectiveness, ease of operation, and cost. The authors concluded that none of the traditional technologies described presented satisfactory results from the environmental point of view and process efficiency. One possible alternative for the treatment of radioactive wastes is their immobilization with a material capable of reducing the possibility of radionuclides being released into the environment, usually Portland cement followed by permanent disposal in a facility with special natural and engineered barriers [6]. However, the high amounts of organics impede an adequate encapsulation of the waste due to the incompatibility with the cement aqueous system [7].

Among efficient processes to degrade organic compounds, there are those called advanced oxidative processes (AOP). These are characterized by the use of hydroxyl radical (•OH), a strong oxidizing species (E^o = 2.80 V EPH) that reacts with second-order kinetics with most organic substances [8]. Moreover, AOPs present low selectivity and

* Corresponding author.
E-mail addresses: lgoulart@alumni.usp.br (L.G.d. Araujo), edu.petraconi@gmail.com (E.S.P. Prado), mirannda.fs@gmail.com (F.d.S. Miranda), rvicente@ipen.br (R. Vicente), argemirosss@gmail.com (A.S.d.S. Sobrinho), petrafilho@gmail.com (G.P. Filho), jtmarumo@ipen.br (J.T. Marumo).

https://doi.org/10.1016/j.jece.2020.104128
Received 18 April 2020; Received in revised form 28 May 2020; Accepted 29 May 2020
Available online 01 June 2020

Table 1
Half-lives of ozone in air and water over the range of temperatures employed in this work and the typical reaction rates of O_3/•OH with a variety of organics. Adapted from [18,19].

Ozone	T (°C)	Half-life (min)
Gas phase	20	4.3×10^3
Aqueous phase	20–30	12–20

Reaction Rates	O_3 (L mol^{-1} s^{-1})	Hydroxyl radical (L mol^{-1} s^{-1})
Phenols	10^{-1}–10^3	10^9–10^{11}
N-containing Organics	10–10^2	10^8–10^{10}
Ketones	1	10^9–10^{10}
Aromatics	1–10^2	10^8–10^{10}
Alcohols	10^{-2}–1	10^8–10^9
Alkanes	10^{-2}	10^6–10^9

velocity close to the limit established by diffusion (second-order rate constant from 10^{10} to 10^{12} mol^{-1} L^{-1}, and stationary concentration between 10^{-10} to 10^{-12} mol L^{-1}, according to [9]. AOPs have been studied for the degradation of oil sludge as a result of the high presence of organics, including processes such as activated persulfate [10] and ozonation [11–13]. Other AOP have been used with an eye toward alter insoluble/solid radioactive waste to less persistent compounds and/or to organic acids that are water-soluble compounds [6,14].

One of the most promising AOP is the ozonation process. Ozone is very reactive and may oxidize various persistent compounds, such as mineral hydrocarbons, and is readily produced when gaseous oxygen is submitted to electrical discharge [15]. Another feature of the ozonation process is that it also generates oxidizing radicals, especially ˙OH, that are formed when ozone decomposes in water [16]. Ozone interaction with matter is namely direct reaction, whereas the interaction of the ozone-generated radicals with matter is namely indirect reaction [17]. Two of the strongest chemical oxidants are ozone and •OH, with high electrochemical potentials (E^o): 2.07 and 2.33 V, respectively.

Table 1 shows that the ozone half-life is greatly influenced by temperature and the physical phase. Furthermore, it shows that the reaction rates are considerably affected depending on the mechanisms involved (direct or indirect reactions) and on the organic compounds present in the target waste.

Ozone has four forms of resonance with varying electrophilic and nucleophilic states. This variety of forms makes ozone an extremely reactive compound [20]. Furthermore, these resonance forms provide contrasting behaviors for ozone. As a result of a delocalized π bond, electrons are given to the atom (nucleophilic, –) and also releases electrons from another (electrophilic, +). This feature is responsible for giving a significantly higher oxidation potential for O_3 (E° = 2.07 V) compared to O_2 (E° = 1.23 V). Note that ozone's solubility is 10–20 times higher than O_2 at room temperature [18,21].

As concerns the reactions of ozone with saturated hydrocarbons, various mechanisms have been actively examined [22]. In these reactions are included those of ozone with C—H bond. There is the direct formation of free radicals (Eqs. (1)–(4)) and also the formation of the transient molecular intermediate-hydrotrioxide ROOOH (Eq. (5)) [18,23].

$$RH + O_3 \rightarrow RO^{\bullet} + HOO^{\bullet} \quad (1)$$

$$RH + O_3 \rightarrow R^{\bullet} + O_2 + {}^{\bullet}OH \rightarrow R{=}O + ROOH \quad (2)$$

$$RH + O_3 \rightarrow RO_2^{\bullet} + {}^{\bullet}OH \quad (3)$$

$$RH + O_3 \rightarrow R^{\bullet} + HO_3^{\bullet} \rightarrow ROH + O_2^{\bullet} \quad (4)$$

$$RH + O_3 \rightarrow R^{\bullet} + HO_3^{\bullet} \rightarrow ROOOH \quad (5)$$

Hydrophilic products are generated as a result of ozone interaction with saturated hydrocarbons, which are ROH, R═O, and ROOH. Considering the H abstraction theory, there is the abstraction of the H atom from the C—H bond by O_3 to produce the HOOO radical. The HOOO radical also abstracts an H atom, thus generating the transient molecular intermediate-hydrotrioxide ROOOH [24–26]. The two H abstractions drive the formation of a double bond. This bond is directly attacked by the O_3 molecule, decomposing HOOOH into H_2O and O_2 [24]. By an equivalent mechanism, the hydrophilic compounds mentioned earlier (ROH, R═O, and ROOH) can be further oxidized by O_3. Nevertheless, the latter reactions have been reported to have much lower kinetics than their precursors. This is due to the stronger electron-withdrawing power of the functional group [27].

Reactions between •OH and saturated hydrocarbons are also present in ozone treatment. This radical is able to oxidize alkanes, branched alkanes, and cycloalkanes, by the H-atom abstraction [28,29]. As expected, the decrease of the C—H bond dissociation energy results in increased rate constants at room temperature. The role of the H-atom abstraction by the •OH is that one hydrogen atom is released by the radical, resulting in the formation of a hydrocarbon radical, as given by Eq. (6) [18]. The hydrocarbon radical is then subject to reactions with O_2 or self-decomposition to form other water-soluble products.

$$R + {}^{\bullet}OH \rightarrow R^{\bullet} + H_2O \quad (6)$$

In this regard, pH is crucial in determining the reaction pathways, since, at low pH, ozone reacts with compounds with particular functional groups. This is a consequence of selective reactions, like those already mentioned, such as electrophilic, nucleophilic, or dipolar addition reaction [30]. On the other hand, at high pH, half of the introduced ozone decomposes into known intermediate oxygen forms and hydroxyl radicals by indirect pathways, which may promote faster degradation of the target pollutant [31].

The present paper investigates the physicochemical modifications of oil sludge treated with several ozone concentrations in the carrier gas, which varied from 13 to 53 mg L^{-1}. Considering that the influence of variation of ozone concentrations on oil sludge degradation was poorly investigated, we now consider a detailed characterization and analysis approach based on modifications of its chemical bonds, absorbance, new species in the oil sludge, and by-products generated and eliminated as gas, and others. For such characterizations, the following techniques were used: Thermal Gravimetric Analysis (TGA), X-ray diffraction (XRD), Scanning Electron Microscopy coupled with Energy-Dispersive X-ray spectrometer (SEM/EDS), Fourier Transform Infrared spectroscopy (FTIR), Spectrophotometry, and Residual Gas Analyzer (RGA).

2. Materials and methods

2.1. Radioactive oil sludge samples

The experiments were conducted with oil sludge generated from Brazilian oil and gas offshore platforms in the Southeast of the country. The oil sludge is conditioned in thousands of drums and some of them were selected for the sampling and, subsequently application of the ozone treatment method. The effect of ozone (with varying concentrations) on the reactions and degradation of oil sludge components was investigated.

2.2. Experimental setup

Fig. 1 illustrates the system used in the experiments. The system is composed of a glass reactor (A) with a capacity of 0.125 L and openings for feeding ozone (B) and sampling (C). For a homogeneous ozone distribution, a glass diffusion plate (D) was positioned at the bottom of the reactor. In the outlet of the reactor a reservoir (E) was placed in the off-gas line to collect any liquid or solid particle carried by the gas flow. A magnetic stirring (F) was used to promote uniform treatment of the samples. Finally, a gas outlet port (G) was used to couple a gas analyzer.

Ozone was generated using the Ozone Solution equipment model VMUS-4 coupled to a Respironics oxygen concentrator model

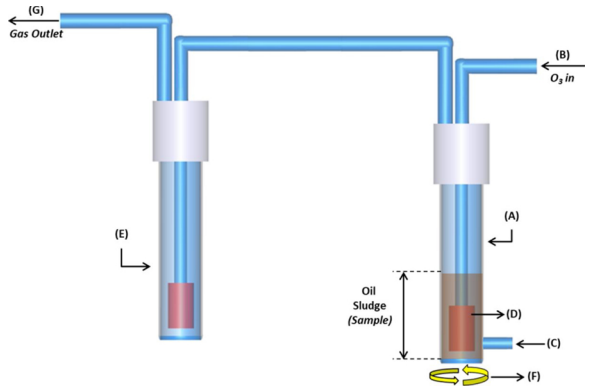

Fig. 1. The experimental setup used in the ozonation experiments. (A) glass reactor with the oil sludge sample; (B) O_3 inlet; (C) sampling point; (D) glass diffusion plate; (E) reservoir; (F) magnetic stirring; and (G) gas outlet.

Table 2
Relationship between oxygen flow and ozone concentration.

Experiment	Flow of O_2 (L min^{-1})	Concentration of O_3 (mg L^{-1})
1	14	13
2	12	23
3	10	33
4	8	43
5	6	53
Control test	10	–

Millenium M10. The variation in the ozone concentration was made by varying the O_2 flow rate between 14–6 L min^{-1} (Table 2). The increase in the flow of O_2 promotes a lower concentration of O_3 and, in the opposite way, the lower flow of O_2 promotes a higher concentration of O_3 [32].

The ozone concentration at the inlet was measured using an ozone gas analyzer (model 106-H, Ozone Solutions). In short, six experimental conditions were carried out, one control (only oxygen) and five ozone concentrations (13, 23, 33, 43, and 53 mg L^{-1}) for 60 min each. In order to verify possible variations, all experiments were made in triplicate (in a total of 18 experiments). The experiments were conducted in batch and, for each experiment, a sample of 0.075 L of oil sludge was treated. Aliquots were collected every 5, 15, 30, 45, and 60 min, for further analyses. Experiments were carried out at pH ~ 6, and no pH adjustments were carried out at the beginning or during the tests. The temperature was monitored during the ozone treatment reaching values between 25–27 °C.

2.3. Materials characterization

Thermal Gravimetric Analysis (TGA) measurements of the oil sludge were performed in nitrogen atmosphere. The experiments were carried out with simultaneous thermal analyzer (Netzsch STA 449 F3 Jupiter) in a temperature range from 30 to 300 °C for the liquid phase and from 30 to 900 °C for the solid phase. The nitrogen flow rate was set at 0.04 L min^{-1} with a heating rate of 30 °C min^{-1}.

X-ray diffraction (XRD) analyses of the solid portion were performed using a PANalytical Empyrean diffractometer with 2θ varying from 15 to 100° with a step size of 0.02°, at room temperature and step time of 10 s.

Sludge samples were dried in an oven at 80 °C and ground for the Scanning Electron Microscopy (SEM) and Energy-dispersive Spectroscopy (EDS) analysis. The analysis was performed in an electron microscopy HITACHI TM3000, with a tungsten source and acceleration voltages of 5 and 15 kV with an electron beam resolution of 30 nm. Images were obtained with magnification from 15 to 30,000 times.

Fourier-transform infrared (FTIR) spectroscopy analyses were performed using a Perkin Elmer Frontier apparatus using universal attenuated total reflectance (UATR) with 16 accumulations. The spectrum was analyzed in the region from 600 to 4000 cm^{-1}. Absorbance was measured using a Shimadzu UV–vis (model 1800) and the software UV-Probe version 2.7; wavelength ranged from 300 to 750 nm. Dilutions (10 ×) were made to the original samples to keep absorbance between 0.1–1.0, to avoid misinterpretations in comparing values of absorbance higher than 1.0.

The composition of the outlet gases for both control and ozonation experiments was analyzed using a Stanford Research Systems model SRS – RGA 200 residual gas analyzer (Fig. 1(G)). Measurements were taken at 2, 30, and 60 min. A control test using only O_2 flow (flow rate: 10 L min^{-1}) was carried out. The objective of this experiment was to trace any loss of compounds in the gas-phase by volatilization and not by the ozone action. The only significant peak observed stood for O_2 (32 *m/z*), indicating that no degradation of the oil sludge had occurred.

3. Results and discussions

3.1. Characterization of the oil sludge prior to the ozone treatments

The characterization of the oil sludge prior to the ozone treatment was performed in the liquid and solid phases. Fig. 2 shows the TGA analysis for the liquid phase (constituted mainly of oil + water) and solid phase as a function of time and temperature.

The mass of the liquid phase started to decrease at approximately 30 °C and reached its maximum removal of about 75 % at approximately 100 °C. It took less than 30 min to reach such degradation, indicating that the liquid phase of the oil sludge contains mainly water and other volatile species, such as H_2S. No significant loss of mass was observed at higher temperatures, from 100 to 300 °C (maximum temperature analyzed for the liquid phase). The residual compounds (25 % of the total mass) were vitrified in a crucible. XRD and EDS spectrum analysis of the material confirmed the presence of barium, as will be shown later on. Under moderate/high temperatures, the barium can solidify in sulfate or oxide forms, which requires temperatures much higher than those utilized for reaching its melting temperature.

The TGA analysis for solid oil sludge highlighted the major presence of inorganic compounds, once only 5 % of mass loss was presented, even for temperatures reaching the 800 °C. This result shows that basically all organics compounds are presented in the liquid phase.

The XRD pattern of the solid part of oil sludge is presented in Fig. 3. The identification of the main diffraction peaks by using the

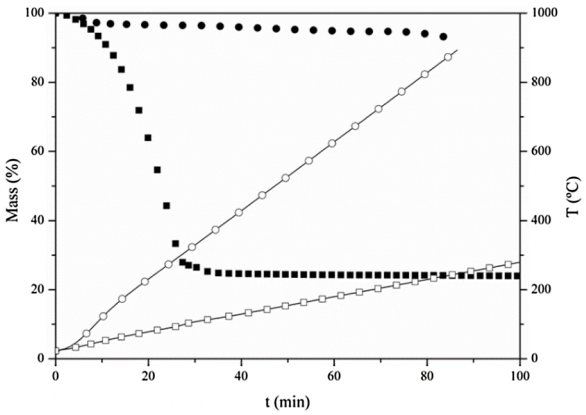

Fig. 2. TGA pyrolysis curves of oil sludge samples. Liquid phase: (black square) mass (%) and (empty square and black line) temperature. Solid-phase: (black round) mass (%), (empty round and black line) temperature. The temperature varied from 30 to 300 °C for the liquid phase and from 30 to 900 °C for the solid phase. The heating rate was 30 °C min^{-1}.

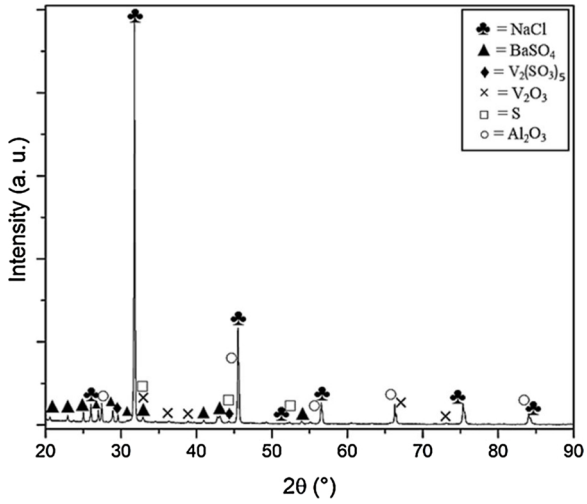

Fig. 3. X-ray diffractogram of the solid part of the Brazilian oil sludge petroleum. 2θ varied from 15 to 100° with a step size of 0.02°, room temperature and step time of 10 s.

HIGHSCORE software. It shows the presence of sodium chloride (NaCl) cubic phase, barium sulfate ($BaSO_4$) in its orthorhombic phase, vanadium sulfite ($V_2(SO_3)_5$) in its hexagonal phase, vanadium oxide (V_2O_3) in its rhombohedral phase, sulfur in its hexagonal phase and aluminum oxide (Al_2O_3) in its cubic phase.

The morphology and the elemental composition of the oil sludge investigated by SEM/EDS analysis are shown in Fig. 4. The solid sample is heterogeneous and it can be noted the presence of the Cl, Ca, O, Ba, Na, S, and Al. These results are in line with those obtained by XRD, which ensures the correct identification of the components of this sample.

The mid-infrared (mid-IR) spectra of the solid and liquid phases that constitute the oil sludge are shown in Fig. 5. It present absorption bands at 3356, 2938, 2924, 2854, 1631, 1458, 1377 cm^{-1} for the liquid phase and 3356, 1651, 1536, 1436, 1103, 1082, 982, 874, 631, and 608 cm^{-1} for the solid phase. The absorption bands located in the 3400–3600 cm^{-1} region were mainly associated with the O—H stretch from water [33,34]. The bands at 2938, 2924, and 2854 cm^{-1} were associated with C—H stretching, C—H in-phase stretch in CH_2, and C—H out-of-phase stretch in CH_2, respectively [33,35–37]. These bands were identified only for the liquid phase.

For both solids and liquids, the band at 1631 cm^{-1} was found and represent the C=C aromatic skeletal stretching [36]. As expected, since the liquid presents a higher presence of organics, the intensity for this peak was more relevant in this phase. The band at 1536 cm^{-1} was detected only for the solid phase. According to Saleh [33], this peak represents the C=C stretching vibration. Therefore, although the liquid portion presented a higher presence of C=C aromatic skeletal stretching, the solid portion presented C=C in its aromatic and non-aromatic forms. The band at 1458 (in the liquid) and 1436 (in the solid) represent the C—H asymmetric deform in CH_2 and CH_3 [33,36].

Finally, the peak 1377 cm^{-1}, for the liquid phase, was identified and corresponds to the C—H symmetric bond. The bands at 1103 cm^{-1} and at 1082 cm^{-1} represent the S—O bond, demonstrating the presence of barite ($BaSO_4$) [38], 982 cm^{-1} was associated with the Si–O stretch and the band at 874 cm^{-1} corresponds to C—O, evidencing the presence of calcite ($CaCO_3$) [39]. The bands 631 and 608 cm^{-1} were associated with SO_4^{2-} bend, that also confirm the occurrence of barite [36].

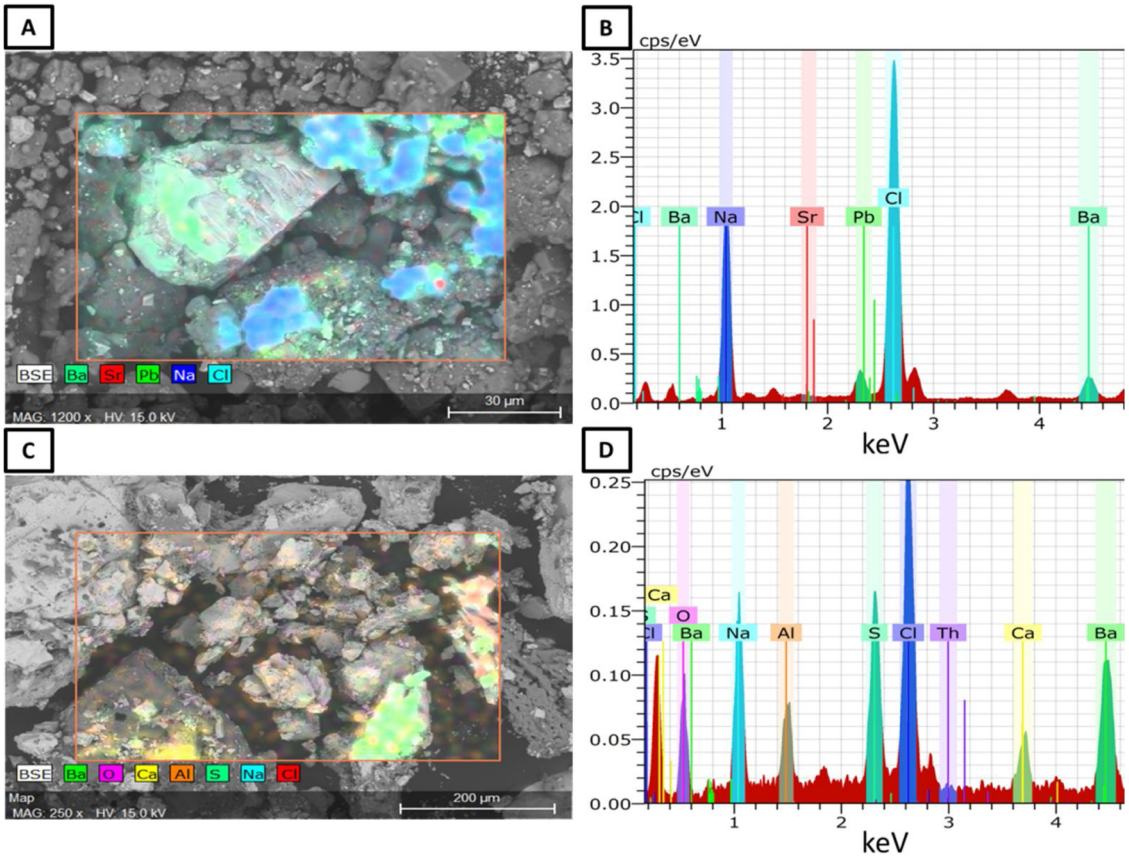

Fig. 4. Micrographs (A, 1200 ×; C, 250 ×) and Energy-dispersive X-ray spectra (B and D) before the oxidation treatment by ozone. Tungsten source, acceleration voltages of 5 and 15 kV, electron beam resolution of 30 nm.

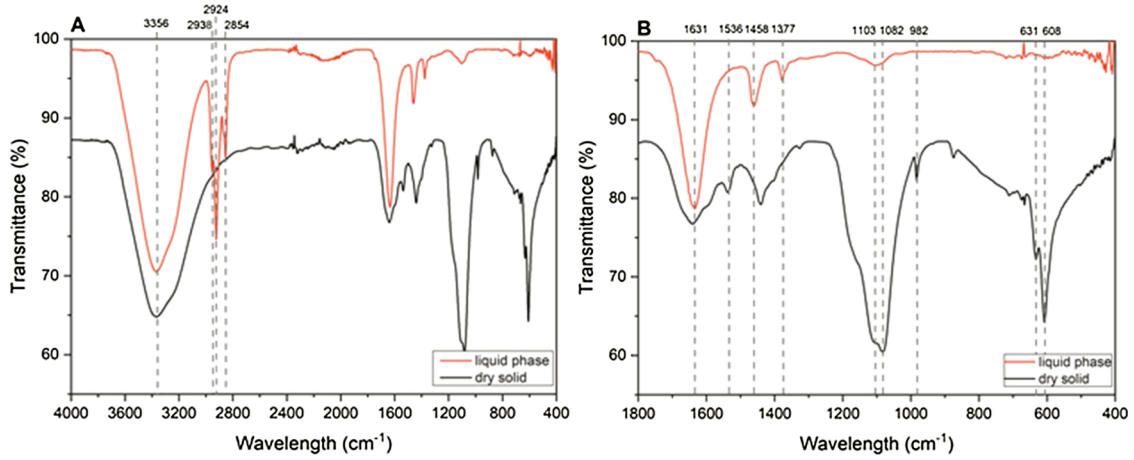

Fig. 5. Mid-IR spectra of the constituents of the oil sludge for liquid phase (red - upper line) and dry solid (black - bottom line). (A) Region 400–4000 cm^{-1}. (B) Magnification of the bands in the region 400–1800 cm^{-1}. UATR with 16 accumulations. (For interpretation of the references to colour in this figure legend, the reader is referred to the web version of this article).

3.2. Characterization of oil sludge after ozonation

The ozonation process promoted considerable differences in the color of the treated solutions indicating the presence of an important oxidation process, as shown in Fig. 6. Note that color changed significantly with the increase of the treatment time and the increase of ozone concentration. It was observed a tendency of a slight decrease in the efficiency in turning clearer the samples treated with higher ozone concentration values, 43 and 53 mg L^{-1}. This must be due to the fact that to increase the ozone concentration we need to decrease the oxygen flow. Then, despite we have a higher ozone concentration we have a small flow of gas interacting with the oil sludge, which decreases the efficiency of the system. In order to improve that, we must have a powerful ozone generator that allows us to increase the ozone concentration keeping constant the oxygen gas flow.

The color changes observed during the oil sludge oxidation process are related to the changes of its composition that consequently changes the solution absorption of the light. Fig. 7 shows the absorbance spectra in the visible range for three ozone treatment concentrations for two different treatment times. The raw oil sludge absorbance is also presented for comparison.

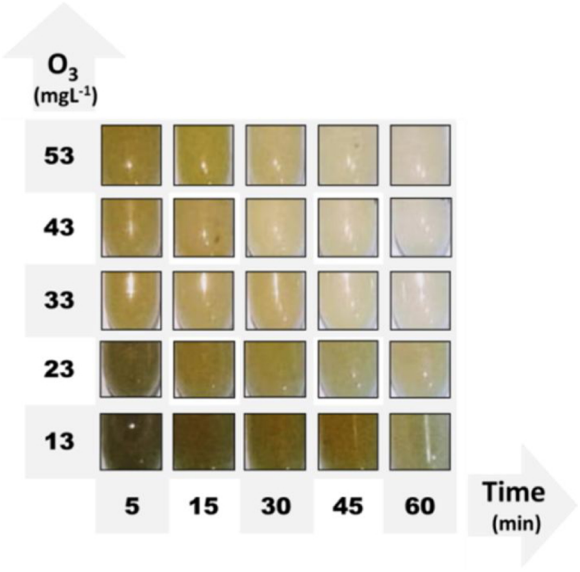

Fig. 6. The color change of the oil sludge samples during the ozone treatment from 5 to 60 min and $[O_3]$ = 13 to 53 mg L^{-1}.

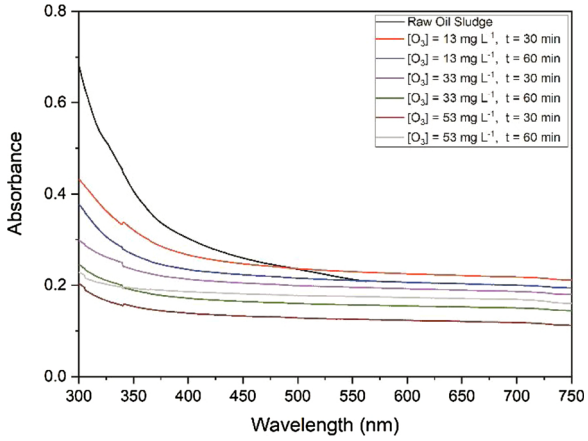

Fig. 7. Absorbance analyses for diluted samples (×10) of the raw oil sludge and after ozone treatment for times 30 and 60 min and ozone concentrations of 13, 33, and 53 mg L^{-1}.

Confirming the visual observation, absorbance decreased with the increase of treatment time and ozone concentration, except for the case of ozone concentration of 53 mg L^{-1}, for reason already mentioned. This result is similar to that observed by [40]. They employed coagulation and ozone catalytic oxidation for pretreating cocking wastewater. As soon as ozone was employed, Chen et al. [40] observed that absorbance values decreased fast, particularly in the range from 300 to 400 nm. According to the authors, the decrease in absorbance is related to the reaction between ozone and the organic compounds. The results here presented indicate that the oxidation process is breaking down the heavy molecular-weight species on the sludge oil in low molecular-weight species as will be shown in the next results.

The mid-IR transmittance spectra of the untreated and ozone-treated oil sludge are shown in Fig. 8. Important changes are observed with the presence of new bands and variation intensities even for only 5 min of ozone treatment. These changes increase in a significant way up to treatment time of 30 min and then decrease for longer treatment times.

The absorption bands located in the 3400–3600 cm^{-1} region, associated with the O—H stretch from water, presented higher intensities after ozone treatment, probably because of the degradation of the organic compounds by mineralization, leading to the formation of CO_2 and H_2O. Many bands disappeared after the ozonation process, which indicated some extent of modification in liquid waste structure. These bands are at 2954, 2923, and 2854 cm^{-1} related to the CH_3 stretching

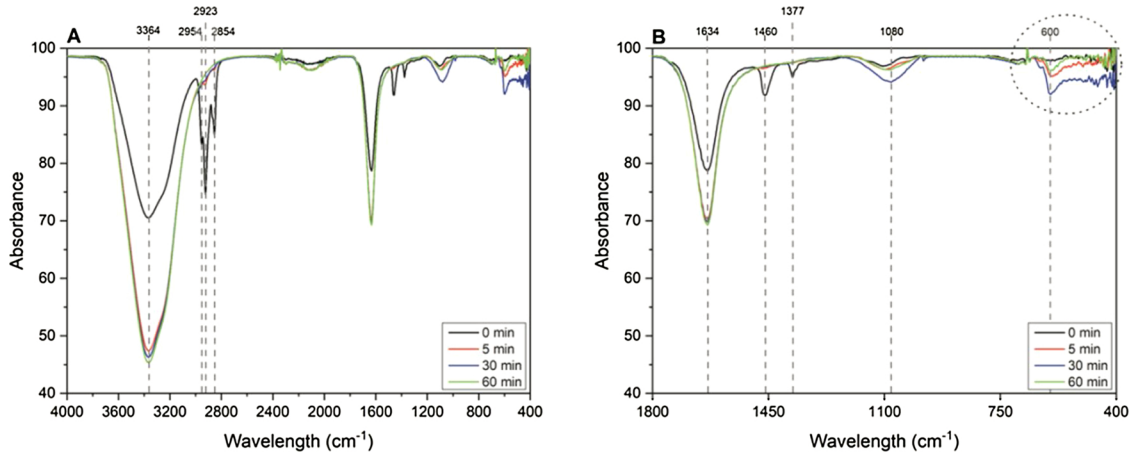

Fig. 8. Mid-IR spectra of the liquid phase of the oil sludge petroleum prior and after ozonation, for selected times (5, 30, and 60 min) and ozone concentration of 53 mg L^{-1}. (a) Region 4000–400 cm^{-1}. (b) Magnification of the bands in the region 1800–400 cm^{-1}.

vibration, C—H in-phase stretch in CH_2, and C—H out-of-phase stretch in CH_2, respectively.

Furthermore, the ozone process promoted a greater presence of C═C aromatic skeletal stretching, as indicated by the increase in the peak band intensity at 1634 cm^{-1}. In this regard, the results, so far, suggest that the by-products formed by the ozonation process may have been formed by the degradation of compounds containing C—H bonds followed by intermediate reactions that resulted in aromatic compounds (C═C aromatic skeletal stretching, 1634 cm^{-1}). The band located at 1460 cm^{-1} (C—H asymmetric deform in CH_2 and CH_3) and at 1377 cm^{-1} (C—H symmetric) also disappeared after treatment. The bands at 1080 and at 600 cm^{-1} may be attributed to the S—O and SO_4^{2-} bends due to the degradation of small solid $BaSO_4$ particles at the bottom of the oil sludge.

As previously mentioned, an ozone gas analyzer was coupled to the gas outlet of the system. Fig. 9 shows the composition of the gases with masses lower than 50 *m/z* produced at 2, 30, and 60 min during the ozonation of the oil sludge.

In the first min of the treatment, the intensity of the peak corresponding to ozone is very low, possibly because almost all ozone injected is reacting with the oil sludge and being consumed in low molecular weight species containing H, C, and S [41]. Organic gases such as CH_2 (14 *m/z*), CH_4 (16 *m/z*), CH_5 (17 *m/z*), C_2H_4 (28 *m/z*), C_2H_5 (29 *m/z*), C_2H_6 (30 *m/z*) and C_3H_4 (40 *m/z*) accounted for the majority of the total gases [42]. Moreover, inorganic gases such as H_2 (4 *m/z*), CO (28 *m/z*), H_2S (34 *m/z*), and CO_2 (44 *m/z*) were also detected.

Although the amounts of the inorganic gases were much lower than those of the organic gases, their significance in the characterization of the ozone interaction with oil sludge could not be ignored. There is a remarkable distinction regarding the presence of C_2H_4 (ethylene, 28 *m/z*) and CO (28 *m/z*) over time in the mass spectra (see Fig. 9). At 2 and 30 min of reaction, the peak identified as ethylene and CO has a high intensity. This is likely due to the combination of these two compounds in the spectra. On the other hand, at 60 min, there is no such peak. Herron and Huie [43] studied the ozone-ethylene reaction and found as intermediates CO, CO_2, H_2, and 2H. Here these intermediates compounds were also found during the reactions between ozone and the oxide matter of the oil sludge (Fig. 9).

As regards H_2S, some researchers have revealed that its generation can be promoted by the catalytic effect of minerals the increase in light hydrocarbons in the exhaust line [44]

The results show that the amount of formed species decreases as the treatment time increases. The spectrum of Fig. 9b clearly shows that after 30 min of treatment, several undefined peaks (low relative intensities) disappeared or significantly reduced. On the other hand, two peaks clearly increased, i.e. CO_2 (44 *m/z*) and O_3 (48 *m/z*). The former

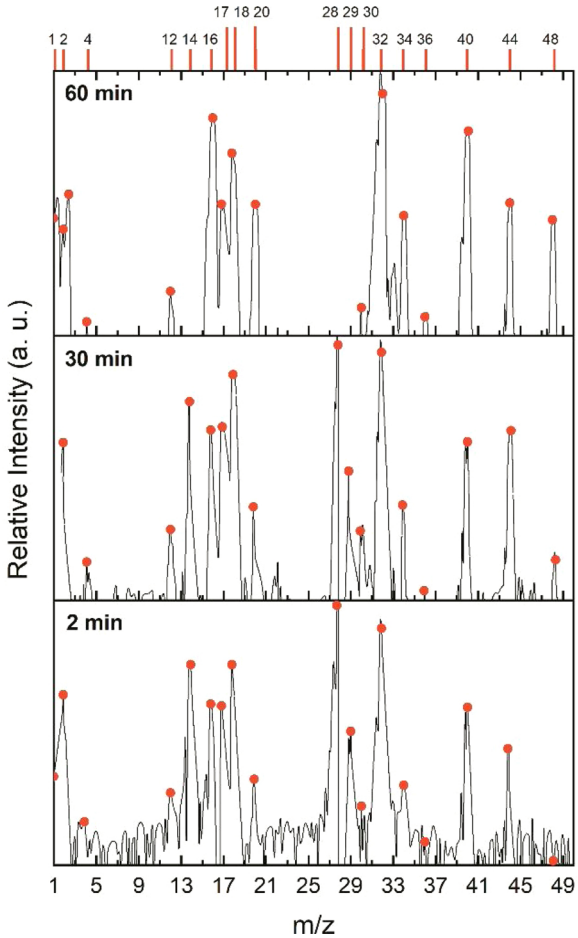

Fig. 9. Mass spectra obtained by residual gas analyzer during the oil sludge ozonation at three different times: 2 min; 30 min; 60 min. $[O_3]$ = 53 mg L^{-1}.

is due to the degradation of organic compounds that are oxidized and mineralized to CO_2 and H_2O [45–47]. The latter indicates that less ozone reacted over time.

The increase in the peak of ozone in the final treatment time of one hour (Fig. 9c) is related to the ozone surplus since almost all organic matter has already been reacted. At this stage, there are still gases being produced from the oxidation process, namely H_2S (34 *m/z*), CO_2 (44 *m/z*), and H_2 (2 *m/z*).

4. Conclusions

The application of ozone with different concentrations (13, 23, 33, 43, and 53 mg L^{-1}) proves to be an effective method of treatment of radioactive oil sludge and was evaluated in the solid, liquid, and gas-phase products during its decomposition. The most visible modification was observed by the different colors of liquid samples during the tests, mainly by the concentration of 33 mg L^{-1}. Therefore, all experimental conditions resulted in a decrease of absorbance with the increase of ozone concentration, as confirmed by spectrophotometric analyses.

The TGA analysis indicated that liquid and solid samples contained about 25% and 5% of non-degradable compounds, respectively. The presence of Cl, Ca, O, Ba, Na, Al, and barium oxide in the solid samples were confirmed by XRD and SEM/EDS analysis.

FTIR spectrometry indicates that ozone promoted alterations in the bonds and structure of the samples. An important formation of CO_2 and H_2O was observed after 5 min of ozone treatment. Organic gases accounted for the majority of the total gases, but inorganic gases such as H_2, CO, CO_2, H, and H_2S were also detected. A saturation of ozone (48 m/z) was observed for a treatment time of 30 min at $[O_3]$ = 53 mg L^{-1} while the amount of ethylene and/or CO (28 m/z) decreases indicating that most oil sludge degradation reaction had already occurred and disappear at 60 min of treatment. The production of CO, CO_2, H_2, and 2H, is probably a result of the degradation of ethylene and other low-chain hydrocarbons present or formed during the process. The catalytic effect that occurred in the sludge was responsible for producing H_2S and partially producing some of the light hydrocarbons presented in the exhaust line.

CRediT authorship contribution statement

Leandro Goulart de Araujo: Conceptualization, Methodology, Validation, Formal analysis, Investigation, Data curation, Writing - original draft, Writing - review & editing, Visualization. **Eduardo Sant'Ana Petraconi Prado:** Conceptualization, Methodology, Validation, Investigation, Formal analysis, Data curation, Writing - original draft. **Felipe de Souza Miranda:** Investigation, Data curation, Writing - original draft, Visualization. **Roberto Vicente:** Conceptualization, Methodology, Writing - review & editing, Supervision. **Argemiro Soares da Silva Sobrinho:** Resources, Writing - review & editing. **Gilberto Petraconi Filho:** Resources, Writing - review & editing, Supervision. **Júlio Takehiro Marumo:** Conceptualization, Methodology, Resources, Writing - review & editing, Supervision, Funding acquisition.

Declaration of Competing Interest

I, Dr. Leandro Goulart de Araujo, on the behalf of the authors whose names are listed in this manuscript submitted to the Journal of Environmental Engineering, **CERTIFY** that they have **NO** affiliations with or involvement in any organization or entity with any financial interest (such as honoraria; educational grants; participation in speakers' bureaus; membership, employment, consultancies, stock ownership, or other equity interest; and expert testimony or patent-licensing arrangements), or non-financial interest (such as personal or professional relationships, affiliations, knowledge or beliefs) in the subject matter or materials discussed in this manuscript.

Acknowledgments

The authors acknowledge the fellowship awarded by the Brazilian National Nuclear Energy Commission to L.G. de Araujo (SEI-IPEN - 01342.002317/2019-91). We also thank the support given by the Center for Lasers and Applications' Multiuser Facility at IPEN-CNEN/SP, the spectrophotometric analyses done by Thalita T. Silva from the Radiation Technology Center at IPEN-CNEN/SP, and the Plasma and Process Laboratory of the Aeronautical Technological Institute (LPP-ITA).

References

[1] E.M. El Afifi, N.S. Awwad, Characterization of the TE-NORM waste associated with oil and natural gas production in Abu Rudeis, Egypt, J. Environ. Radioact. 82 (2005) 7–19, https://doi.org/10.1016/j.jenvrad.2004.11.001.
[2] K. Al Nabhani, F. Khan, M. Yang, Technologically enhanced naturally occurring radioactive materials in oil and gas production: a silent killer, Process Saf. Environ. Prot. 99 (2016) 237–247, https://doi.org/10.1016/j.psep.2015.09.014.
[3] M.F. Attallah, M.M. Hamed, E.M.A. El, H.F. Aly, Removal of ^{226}Ra and surfactants solutions Ra from TENORM sludge waste using, J. Environ. Radioact. 139 (2015) 78–84, https://doi.org/10.1016/j.jenvrad.2014.09.009.
[4] B. Islam, Petroleum sludge, its treatment and disposal: a review, Int. J. Chem. Sci. 13 (2015) 1584–1602.
[5] G. Jing, M. Luan, W. Du, Treatment of oily sludge by advanced oxidation process, Environ. Earth Sci. 67 (2012) 2217–2221, https://doi.org/10.1007/s12665-012-1662-7.
[6] L. de Araujo, J. Marumo, Reaction of ion exchange resins with Fenton's reagent, Environments 5 (2018) 123, https://doi.org/10.3390/environments5110123.
[7] O. Gorbunova, A. Safonov, V. Tregubova, K. German, Cementation of biodegraded radioactive oils and organic waste, J. Radioanal. Nucl. Chem. 304 (2015) 371–375, https://doi.org/10.1007/s10967-014-3887-2.
[8] T. Wang, Z.X. Huang, H.F. Miao, W.Q. Ruan, X.P. Ji, F.B. Sun, M.X. Zhao, H.Y. Ren, Insights into influencing factor, degradation mechanism and potential toxicity involved in aqueous ozonation of oxcarbazepine (CHEM46939R1), Chemosphere 201 (2018) 189–196, https://doi.org/10.1016/j.chemosphere.2018.02.062.
[9] T. Oppenländer, Photochemical Purification of Water and Air: Advanced Oxidation Processes (AOPs)-principles, Reaction Mechanisms, Reactor Concepts, John Wiley & Sons, 2007, https://doi.org/10.1017/CBO9781107415324.004.
[10] B. Desalegn, M. Megharaj, Z. Chen, R. Naidu, Green mango peel-nanozerovalent iron activated persulfate oxidation of petroleum hydrocarbons in oil sludge contaminated soil, Environ. Technol. Innov. 11 (2018) 142–152, https://doi.org/10.1016/J.ETI.2018.05.007.
[11] C. Chen, X. Yan, Y. Xu, B.A. Yoza, X. Wang, Y. Kou, H. Ye, Q. Wang, Q.X. Li, Activated petroleum waste sludge biochar for efficient catalytic ozonation of refinery wastewater, Sci. Total Environ. 651 (2019) 2631–2640, https://doi.org/10.1016/J.SCITOTENV.2018.10.131.
[12] M. Gozan, Oil Extraction From Oil Sludge and TPH Elimination of Solids/Water by Ozonation, Energy Environ. Res. 4 (2014) 22–28, https://doi.org/10.5539/eer.v4n2p22.
[13] T.S. Kwon, J.Y. Lee, Options for reducing oil content of sludge from a petroleum wastewater treatment plant, Waste Manag. Res. 33 (2015) 937–940, https://doi.org/10.1177/0734242X15597776.
[14] Z. Wan, L. Xu, J. Wang, Treatment of spent radioactive anionic exchange resins using Fenton-like oxidation process, Chem. Eng. J. (2016), https://doi.org/10.1016/j.cej.2015.09.004.
[15] E. Latini, E. Curci, A. Massimiani, S. Nusca, F. Santoboni, D. Trischitta, M. Vetrano, M. Vulpiani, Ultrasonography for oxygen-ozone therapy in musculoskeletal diseases, Med. Gas Res. 9 (2019) 18–23, https://doi.org/10.4103/2045-9912.254638.
[16] P.A. Morozov, B.G. Ershov, The influence of phosphates on the decomposition of ozone in water: chain process inhibition, Russ. J. Phys. Chem. A 84 (2010) 1136–1140, https://doi.org/10.1134/S0036024410070101.
[17] M.A. Malik, A. Ghaffar, Water purification by electrical discharges, Plasma Sources Sci T 10 (2001).
[18] T. Chen, Applying Ozone to Accelerate Remediation of Petroleum-Contaminated Soils, Arizona State University, 2018.
[19] A.A. Gonçalves, Ozone - an emerging technology for the seafood industry, Braz. Arch. Biol. Technol. 52 (2009) 1527–1539, https://doi.org/10.1590/S1516-89132009000600025.
[20] F.J. Beltrán, Ozone Reaction Kinetics of Water and Wastewater Systems, (2003).
[21] G. Miller, An Assessment of Ozone and Chlorine Dioxide Technologies for Treatment of Municipal Water Supplies Vol. 1 Environmental Protection Agency, Office of Research and Development, Municipal Environmental Research Laboratory, 1978, p. 68.
[22] P.S. Bailey, Ozonation in Organic Chemistry, (1982), https://doi.org/10.1016/b978-0-12-073102-2.x5001-0.
[23] Q.K. Timerghazin, S.L. Khursan, V.V. Shereshovets, Theoretical study of the reaction between ozone and C–H bond: gas-phase reactions of hydrocarbons with ozone, J. Mol. Struct. Theochem. 489 (1999) 87–93, https://doi.org/10.1016/S0166-1280(99)00081-0.
[24] J. Cerkovnik, E. Eržen, J. Koller, B. Plesničar, Evidence for HOOO radicals in the formation of alkyl hydrotrioxides (ROOOH) and hydrogen trioxide (HOOOH) in the ozonation of C–H bonds in hydrocarbons, J. Am. Chem. Soc. 124 (2002) 404–409, https://doi.org/10.1021/ja017320i.
[25] B. Plesničar, J. Cerkovnik, T. Tuttle, E. Kraka, D. Cremer, Evidence for the $HOOO^-$ anion in the ozonation of 1,3-dioxolanes: Hemiortho esters as the primary products, J. Am. Chem. Soc. 124 (2002) 11260–11261, https://doi.org/10.1021/ja0276319.
[26] R. Lee, M.L. Coote, Mechanistic insights into ozone-initiated oxidative degradation of saturated hydrocarbons and polymers, Phys. Chem. Chem. Phys. 18 (2016) 24663–24671, https://doi.org/10.1039/c6cp05064f.
[27] C. von Sonntag, U. von Gunten, Chemistry of Ozone in Water and Wastewater

Treatment, (2012), https://doi.org/10.2166/9781780400839.
[28] N.R. Greiner, Hydroxyl radical kinetics by kinetic spectroscopy. VI. Reactions with Alkanes in the range 300–500 K, J. Chem. Phys. 53 (1970) 1070–1076, https://doi.org/10.1063/1.1674099.
[29] T. Hashimoto, S. Iwata, Theoretical study on the weakly-bound complexes in the reactions of hydroxyl radical with saturated hydrocarbons (methane, ethane, and propane), J. Phys. Chem. A 106 (2002) 2652–2658, https://doi.org/10.1021/jp0131572.
[30] S.K. Tripathi, N.K. Bhardwaj, H. Roy Ghatak, Developments in ozone-based bleaching of pulps, Ozone Sci. Eng. 42 (2020) 194–210, https://doi.org/10.1080/01919512.2019.1647407.
[31] J. Farkas, M. Náfrádi, T. Hlogyik, B. Cora Pravda, K. Schrantz, K. Hernádi, T. Alapi, Comparison of advanced oxidation processes in the decomposition of diuron and monuron-efficiency, intermediates, electrical energy per order and the effect of various matrices, Environ. Sci. Water Res. Technol. 4 (2018) 1345–1360, https://doi.org/10.1039/c8ew00202a.
[32] G. Xiong, J.A. Koziel, J. Pawliszyn, Air sampling of aromatic hydrocarbons in the presence of ozone by solid-phase microextraction, J. Chromatogr. A 1025 (2004) 57–62, https://doi.org/10.1016/j.chroma.2003.10.078.
[33] T.A. Saleh, Simultaneous adsorptive desulfurization of diesel fuel over bimetallic nanoparticles loaded on activated carbon, J. Clean. Prod. 172 (2018) 2123–2132, https://doi.org/10.1016/j.jclepro.2017.11.208.
[34] T.A. Saleh, M. Tuzen, A. Sarı, Magnetic vermiculite-modified by poly(trimesoyl chloride-melamine) as a sorbent for enhanced removal of bisphenol A, J. Environ. Chem. Eng. 7 (2019) 103436, https://doi.org/10.1016/j.jece.2019.103436.
[35] M. Poletto, V. Pistor, A. J, Structural characteristics and thermal properties of native cellulose, Cellul. - Fundam. Asp. (2013), https://doi.org/10.5772/50452.
[36] S. Cheng, A. Li, K. Yoshikawa, High quality oil recovery from oil sludge employing a pyrolysis process with oil sludge ash catalyst, Int. J. Waste Resour. 05 (2015).
[37] T.A. Saleh, Nanocomposite of carbon nanotubes/silica nanoparticles and their use for adsorption of Pb(II): from surface properties to sorption mechanism, Desalin, Water Treat. 57 (2016) 10730–10744, https://doi.org/10.1080/19443994.2015.1036784.
[38] P.F. Andrade, T.F. Azevedo, I.F. Gimenez, A.G.S. Filho, L.S. Barreto, Conductive carbon-clay nanocomposites from petroleum oily sludge, J. Hazard. Mater. 167 (2009) 879–884, https://doi.org/10.1016/j.jhazmat.2009.01.070.
[39] A.P. Dos Santos Pereira, M.H.P. Da Silva, É.P. Lima, A. Dos Santos Paula, F.J. Tommasini, Processing and characterization of PET composites reinforced with geopolymer concrete waste, Mater. Res. 20 (2017) 411–420, https://doi.org/10.1590/1980-5373-MR-2017-0734.
[40] L. Chen, Y. Xu, Y. Sun, Combination of coagulation and ozone catalytic oxidation for pretreating coking wastewater, Int. J. Environ. Res. Public Health 16 (2019) 1705, https://doi.org/10.3390/ijerph16101705.
[41] S.D. Razumovskii, M.L. Konstantinova, T.V. Grinevich, G.V. Korovina, V.Y. Zaitsev, Mechanism and kinetics of the reaction of ozone with sodium chloride in aqueous solutions, React. Kinet. Catal. Lett. 51 (2010) 492–496, https://doi.org/10.1134/S0023158410040051.
[42] G.T. Tellez, N. Nirmalakhandan, J.L. Gardea-Torresdey, Performance evaluation of an activated sludge system for removing petroleum hydrocarbons from oilfield produced water, Adv. Environ. Res. 6 (2002) 455–470, https://doi.org/10.1016/S1093-0191(01)00073-9.
[43] J.T. Herron, R.E. Huie, Stopped-Flow Studies of the Mechanisms of Ozone-Alkene Reactions in the Gas Phase. Ethylene, J. Am. Chem. Soc. 99 (1977) 5430–5435, https://doi.org/10.1021/ja00458a033.
[44] Q. Ma, Z. Yang, L. Zhang, R. Lin, X. Wang, Generation of hydrogen sulfide during the thermal enhanced oil recovery process under superheated steam conditions, RSC Adv. 9 (2019) 33990–33996, https://doi.org/10.1039/c9ra07735a.
[45] A. Xu, L. Mu, Z. Fan, X. Wu, L. Zhao, B. Bo, T. Xu, Mechanism of heavy oil recovery by cyclic superheated steam stimulation, J. Pet. Sci. Eng. 111 (2013) 197–207, https://doi.org/10.1016/j.petrol.2013.09.007.
[46] A. Bernal-Martínez, H. Carrère, D. Patureau, J.P. Delgenès, Combining anaerobic digestion and ozonation to remove PAH from urban sludge, Process Biochem. 40 (2005) 3244–3250, https://doi.org/10.1016/j.procbio.2005.03.028.
[47] L. Goulart de Araujo, Fda S. Santos, A.C.S.C. Teixeira, Degradation of bisphenol A by the UV and UV/H_2O_2 processes: evaluation of process variables through experimental design, Can. J. Chem. Eng. 95 (2017) 2278–2285, https://doi.org/10.1002/cjce.22997.